Cross-section imaging and p-type doping assessment of ZnO/ZnO:Sb core-shell nanowires by scanning capacitance microscopy and scanning spreading resistance microscopy

Lin Wang, Vincent Sallet, Corinne Sartel, Georges Bremond

▶ **To cite this version:**

Lin Wang, Vincent Sallet, Corinne Sartel, Georges Bremond. Cross-section imaging and p-type doping assessment of ZnO/ZnO:Sb core-shell nanowires by scanning capacitance microscopy and scanning spreading resistance microscopy. Applied Physics Letters, 2016, 109 (9), pp.092101. 10.1063/1.4962046 . hal-02073077

HAL Id: hal-02073077
https://hal.science/hal-02073077

Submitted on 10 Dec 2021

HAL is a multi-disciplinary open access archive for the deposit and dissemination of scientific research documents, whether they are published or not. The documents may come from teaching and research institutions in France or abroad, or from public or private research centers.

L'archive ouverte pluridisciplinaire **HAL**, est destinée au dépôt et à la diffusion de documents scientifiques de niveau recherche, publiés ou non, émanant des établissements d'enseignement et de recherche français ou étrangers, des laboratoires publics ou privés.

AIP | Applied Physics Letters

Cross-section imaging and p-type doping assessment of ZnO/ZnO:Sb core-shell nanowires by scanning capacitance microscopy and scanning spreading resistance microscopy

Lin Wang, Vincent Sallet, Corinne Sartel, and Georges Brémond

Citation: Applied Physics Letters **109**, 092101 (2016); doi: 10.1063/1.4962046
View online: http://dx.doi.org/10.1063/1.4962046
View Table of Contents: http://scitation.aip.org/content/aip/journal/apl/109/9?ver=pdfcov
Published by the AIP Publishing

Articles you may be interested in

Access to residual carrier concentration in ZnO nanowires by calibrated scanning spreading resistance microscopy
Appl. Phys. Lett. **108**, 132103 (2016); 10.1063/1.4945100

Opto-electrical properties of Sb-doped p-type ZnO nanowires
Appl. Phys. Lett. **104**, 111909 (2014); 10.1063/1.4869355

Aluminum doped core-shell ZnO/ZnS nanowires: Doping and shell layer induced modification on structural and photoluminescence properties
J. Appl. Phys. **114**, 134307 (2013); 10.1063/1.4824288

Optical evidence for donor behavior of Sb in ZnO nanowires
Appl. Phys. Lett. **102**, 132105 (2013); 10.1063/1.4799385

ZnO homojunction photodiodes based on Sb-doped p-type nanowire array and n-type film for ultraviolet detection
Appl. Phys. Lett. **98**, 041107 (2011); 10.1063/1.3551628

Reuse of AIP Publishing content is subject to the terms at: https://publishing.aip.org/authors/rights-and-permissions. Download to IP: 193.51.38.25 On: Tue, 30 Aug 2016 08:43:15

Cross-section imaging and p-type doping assessment of ZnO/ZnO:Sb core-shell nanowires by scanning capacitance microscopy and scanning spreading resistance microscopy

Lin Wang,[1,a)] Vincent Sallet,[2] Corinne Sartel,[2] and Georges Brémond[1]
[1]*Institut des Nanotechnologies de Lyon (INL), Université de Lyon, CNRS UMR 5270, INSA Lyon, Bat. Blaise Pascal, 7 Avenue, Jean Capelle, 69621 Villeurbanne, France*
[2]*Groupe d'étude de la Matière Condensée (GEMaC), CNRS - Université de Versailles St Quentin en Yvelines, Université Paris-Saclay, 45 Avenue des Etats-Unis, 78035 Versailles, France*

(Received 3 June 2016; accepted 13 August 2016; published online 29 August 2016)

ZnO/ZnO:Sb core-shell structured nanowires (NWs) were grown by the metal organic chemical vapor deposition method where the shell was doped with antimony (Sb) in an attempt to achieve ZnO p-type conduction. To directly investigate the Sb doping effect in ZnO, scanning capacitance microscopy (SCM) and scanning spreading resistance microscopy (SSRM) were performed on the NWs' cross-sections mapping their two dimensional (2D) local electrical properties. Although no direct p-type inversion in ZnO was revealed, a lower net electron concentration was pointed out for the Sb-doped ZnO shell layer with respect to the non-intentionally doped ZnO core, indicating an evident compensating effect as a result of the Sb incorporation, which can be ascribed to the formation of Sb-related acceptors. The results demonstrate SCM/SSRM investigation being a direct and effective approach for characterizing radial semiconductor one-dimensional (1D) structures and, particularly, for the doping study on the ZnO nanomaterial towards its p-type realization. *Published by AIP Publishing*. [http://dx.doi.org/10.1063/1.4962046]

ZnO is considered as a promising material for optoelectronic applications such as light-emitting diodes (LEDs), ultraviolet lasers/sensors, and dye-sensitized solar cells.[1–4] Nevertheless, the development of these ZnO-based applications has long been bottlenecked by the lack of ZnO p-type doping in terms of reliability and reproducibility.[5] The difficulty of doping ZnO into p-type has been ascribed to the unintentional native donor defects (oxygen vacancy V_O and zinc interstitial Zn_i), hydrogen donors, deep acceptor levels, and low solubility of the acceptor dopants.[6–9] Recently, ZnO nanowires (NWs) have attracted increasing attention and are considered as the building blocks for diverse future functional devices at the nanoscale.[2–4,10,11] In the ZnO NWs' doping study, one particular issue is their electrical characterization, including the determination of free carrier type and mobility. Especially, the study on doping behavior usually involves the characterization of electrical property dependence on varying growth and doping conditions, which is essential for finding the optimal parameters for ZnO p-type realization. Unlike 2D materials, whose electrical properties can readily be investigated by the Hall measurement, electrical characterization on NWs regularly relies on a single NW field effect transistor (FET) structure, involving the complicated photo- (or electron beam) lithography and patterning process.[12–15] Furthermore, this method does not allow individually the electrical assessment of each component inside multilayered 1D structures, for instance, core-shell NWs. The recently developed Hall effect measurement on individual NWs is able to investigate the core-shell NW structure but also requires particular lithography process.[15,16]

In the last two decades, scanning capacitance microscopy (SCM) and scanning spreading resistance microscopy (SSRM) have emerged as two powerful techniques for 2D semiconductor electrical properties mapping with a nanometer-scale spatial resolution.[17–19] In SCM, the metal-coated tip and the sample form a metal-insulator-semiconductor (MIS) structure. Under a modulation alternating voltage (V_{ac}) at tens of kilohertz (kHz) frequency, the variation of the tip/sample capacitance (usually called dC/dV) is stimulated and detected using an ultra-high frequency (~1 GHz) capacitance sensor in combination with a lock-in amplifier, which is directly correlated with the local free carrier concentration and its type of the sample underneath the tip.[17] Typically, the dC/dV signal amplitude is related to free carrier density (a material with a lower carrier density is more easily depleted thus giving rise to a larger dC/dV amplitude), whereas the dC/dV signal phase reflects the carrier type because electrons and holes respond oppositely to the modulating voltage. In contrast, SSRM applies a direct voltage (V_{dc}) on the tip/sample system and measures the electrical resistance which, in the ideal case, is dominated by the local spreading resistance of the sample, enabling SSRM for 2D resistivity/carrier profiling.[18]

In the previous work, we have demonstrated SCM and SSRM being suitable tools for carrier profiling in nanoscaled ZnO materials.[20,21] In this work, we present an alternative practicable approach to study the impurity doping effect in ZnO by performing SCM and SSRM investigation on the specially grown ZnO/ZnO:Sb core-shell NW structure. It shows that the core-shell structure in combination with SCM/SSRM can be a good way to study and achieve acceptor doping in ZnO.

a)E-mail: lin.wang@insa-lyon.fr

Reuse of AIP Publishing content is subject to the terms at: https://publishing.aip.org/authors/rights-and-permissions. Download to IP: 193.51.38.25 On: Tue, 30 Aug 2016 08:43:15

We have chosen antimony (Sb) as the dopant for ZnO considering that over the last few years, p-type conductivity or acceptor incorporation has been reported on Sb doped ZnO, suggesting Sb being a good candidate for ZnO p-type realization.[22–24] ZnO/ZnO:Sb core/shell NWs along the c-axis were grown at 900 °C in a horizontal MOCVD reactor operating at 50 Torr following a two-step process. ZnO NWs were previously deposited on A-sapphire using diethylzinc (DEZn) and nitrous oxide (N_2O) as zinc and oxygen precursors, respectively. Then, in a second run, Sb doped layers were grown on ZnO NWs with triethylantimony (TESb) serving as the Sb-doping source. The TESb flow was 0.008 μmol/min. The transition in the growth regime, i.e., the transition between 1D growth for the core and 2D layer for the shell, was controlled by the N_2O/DEZn partial pressure ratio ($R_{VI/II}$). Smooth thin films were obtained using high $R_{VI/II}$, above 5000, whereas NWs were grown with an O/Zn ratio around 800.

Figure 1 shows scanning electron microscopy (SEM) images of the NWs. The as-grown non-intentionally doped (nid) core ZnO NWs exhibit a length of near 4 μm and a diameter range of 70–130 nm (Figure 1(a)). The subsequent growth of the ZnO:Sb layer resulted in a core-shell structure with a similar length to the original ZnO NWs and an increased diameter in the range of 300–450 nm, as shown in Figure 1(b)). This core-shell configuration will allow for a more reliable quantitative analysis between the two parts of the NWs, with respect to the case of two separated samples. To give an estimation of the Sb content inside the shell layer, the SIMS measurement on a 2D ZnO:Sb film that was grown on sapphire at the same time has revealed an Sb concentration of $6 \times 10^{19}\,cm^{-3}$. To carry out SCM and SSRM measurements on the NWs' cross-sections, the sample was prepared following a procedure described in our previous work,[21] which primarily consisted of dip-coating of SiO_2 and chemical mechanical polishing (CMP). Large area silver paint was used to form metallic contact with the sample's seed layer as well as the top of a large number of NWs.[25] All the SCM and SSRM measurements were conducted in air using a scanning probe microscope (Digital Instruments Dimension 3100) equipped with suitable electrical modules. Probe tips were commercial Pt/Ir coated Si tips for SCM and conductive diamond coated Si tips for SSRM. All the voltages were applied on the sample while the tip was grounded. An illustration of the SCM/SSRM measurements on the prepared NW sample is shown in Figure 1(c).

It is worth emphasizing that because actual flat-band voltage between the tip and sample surface is not well known in most cases, for reasonable carrier mapping by SCM, multiple values of V_{dc} should be used in order to find out the largest dC/dV amplitude, which can be interpreted for obtaining carriers information of interest.[20,26] So SCM was performed with a series of V_{dc} and the used V_{ac} was 1000 mV at a frequency of 50 kHz. Typical results on the ZnO/ZnO:Sb core-shell NW are presented in Figure 2. The investigated area has a roughness with a root-mean-square (RMS) value of ~0.87 nm and the height difference between the core and the shell is less than 3 nm (Figure 2(a)). SCM images under various V_{dc} between −1 and 1 V with 0.5 V step are shown in Figures 2(b)–2(f). For straightforward comparison, they share the same color scale of dC/dV amplitude as in Figure 2(b). As can be seen, the SCM response of the NWs displays a dependence on V_{dc}, an usual phenomenon in SCM imaging, and the strongest signal is obtained at $V_{dc} = 0$ V where a clear contrast is observable between the core and the shell areas. This result manifests unambiguously that the nid ZnO core exhibits a higher free carrier density in comparison to the ZnO:Sb shell. Additionally, from the dC/dV phase image in Figure 2(g), no opposite polarities of the phase signal are observed for the NW, indicating that the shell of the NW is of the same conduction type (n-type) as the core part. Although accurate quantitative analysis of the SCM result in terms of carrier concentration is still rather difficult due to the complicated 3D model and the requirement of many parameters regarding the tip geometry, the sample surface conditions, and/or a lack of calibration dataset,[27] we could estimate the Sb doping effect according to our previous results on nid ZnO NWs and the SCM theoretical model established by Ruda and Shik.[28] In Ref. 28, it has been theoretically analysed that in the depletion regime, the slope of the linear $(dC/dV)^{-2}$ versus V dependence is proportional to the doping concentration and can be used for its determination. From the dC/dV amplitude profiles in Figure 2(h), its values for the NW core at $V_{dc} = 0.5$ V and 1 V are around 170 mV and 30 mV, respectively. The corresponding values for the NW shell are 300 mV and 150 mV for $V_{dc} = 0.5$ V and 1 V, respectively. Then, according to the conclusion in Ref. 28, the carrier density ratio between the core and the shell can be determined to be on the order of 30.

Two previous separate studies, i.e., four-probe measurements[29] and calibrated SSRM,[21] have revealed a residual n-type carrier concentration around $2 \times 10^{18}\,cm^{-3}$ for ZnO NWs grown under similar conditions. Assuming it is still the case for the ZnO core in this work, (i.e., $n_{core} \approx 2 \times 10^{18}\,cm^{-3}$), then the carrier concentration in the ZnO:Sb part can be estimated to be $\sim 7 \times 10^{16}\,cm^{-3}$. This result indicates that with a total Sb doping concentration of about $6 \times 10^{19}\,cm^{-3}$, the residual free electron concentration is lowered by more than one order of magnitude (from $\sim 2 \times 10^{18}\,cm^{-3}$ to $\sim 7 \times 10^{16}\,cm^{-3}$), which is a clear proof of the electrical compensation effect

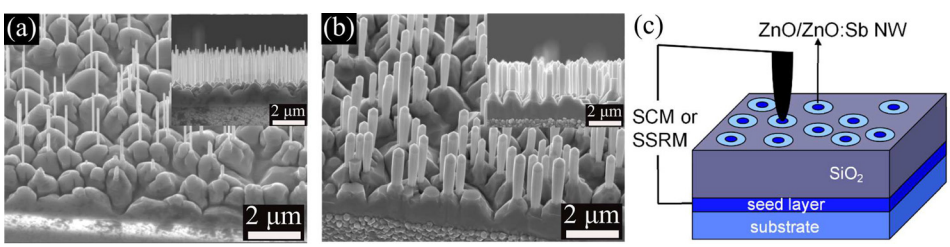

FIG. 1. (a) SEM tilt view and side view (inset) of the as-grown ZnO core NWs. (b) SEM tilt view and side view (inset) after the growth of the ZnO:Sb shell layer. (c) An illustration of the SCM/SSRM measurement on the NWs after the preparation process.

Reuse of AIP Publishing content is subject to the terms at: https://publishing.aip.org/authors/rights-and-permissions. Download to IP: 193.51.38.25 On: Tue, 30 Aug 2016 08:43:15

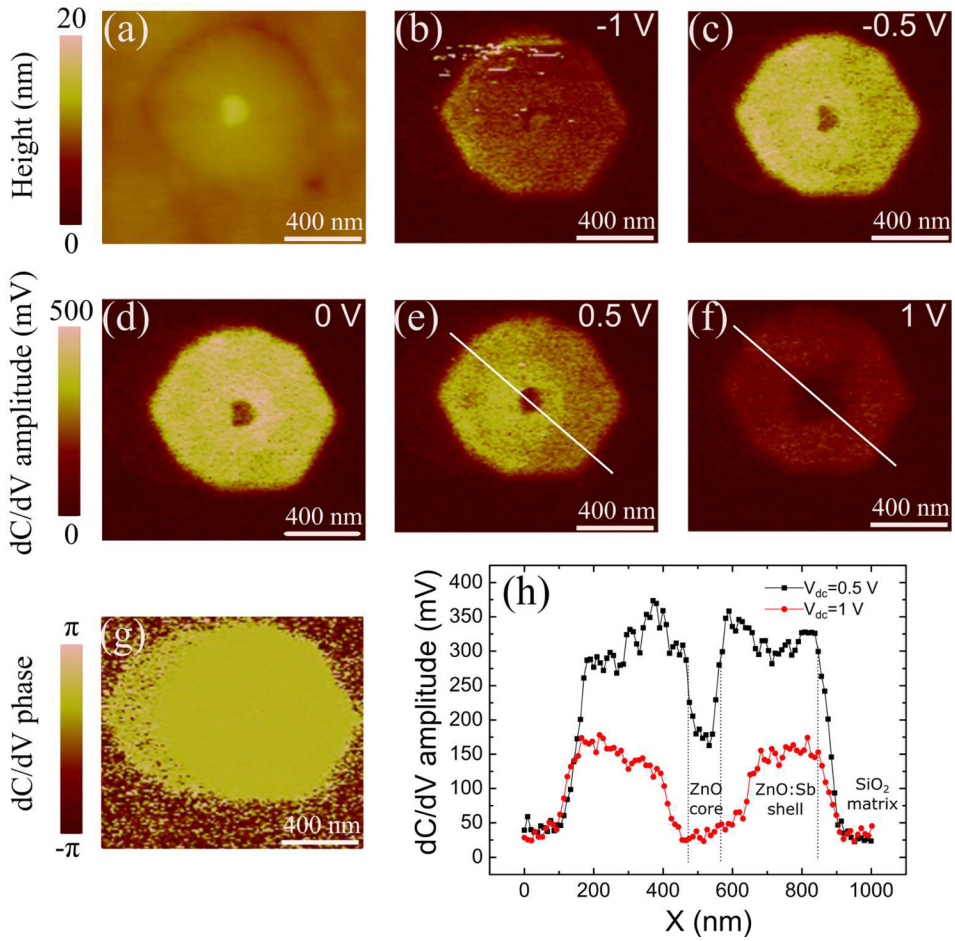

FIG. 2. SCM results on a NW with the ZnO/ZnO:Sb core-shell structure. (a) Topography image with a roughness RMS value ~0.87 nm. (b)–(f) dC/dV amplitude image at a series of V_{dc} (−1 V, −0.5 V, 0 V, 0.5 V, and 1 V). (g) dC/dV phase image. The whole NW is identified being of n-type conductivity. (h) dC/dV amplitude profiles along the lines marked in (e) and (f). Note that dC/dV amplitude images (b)–(f) share the same color scale on the left side of (d).

induced by the Sb incorporation in the ZnO shell. Here, we remind that due to the SCM signal noise as well as the distance of the theoretical model from the real measurement, a large uncertainty may exist for the obtained carrier density value, which is still a main limiting problem for the application of the SCM technique and needs to be improved. Furthermore, although the Debye length is small (less than 1 nm for $10^{18}\,cm^{-3}$), due to the small size of the NW core and the finite size of the tip, especially when tip wear occurs, the overlap of the tip on the shell region (even without direct contact where air will play the role of the insulating layer) can have an effect on the SCM result for the core region, giving rise to a higher dC/dV amplitude than representative for its real carrier density. In this regard, a larger difference of the dC/dV signal and thus carrier densities between the core and the shell might be expected.

Figure 3 shows a representative SSRM measurement result on the same sample. From the topography image in Figure 3(a), the NWs can be recognized and the core of them can also be distinguished from their shells. The SSRM resistance image was acquired simultaneously and is given in Figure 3(b). Evidently, a core-shell contrast is resolved indicating a difference in SSRM resistance during the tip scan on the ZnO cores and the ZnO:Sb shells. In order to better display this contrast, a profile along the line indicated in Figure 3(c) is presented in Figure 3(d). It is found that the resistance for the core is on the order of $5 \times 10^5\ \Omega$ whereas the shell part corresponds to values $\sim 3 \times 10^8\ \Omega$, almost 3 orders of magnitude larger, implying a much higher resistivity in the ZnO:Sb part of the NW. The higher resistivity corresponding to the ZnO:Sb shell layer can be interpreted by both an electrical compensation of ZnO residual carrier concentration and a decrease of the carrier mobility due to high-level Sb atoms incorporation.[30]

Thus, SCM and SSRM have experimentally imaged the cross-sections of our 1D structures. With SCM having the ability to differentiate between n- and p-type conductivity, the results show that no p-type inversion was achieved after Sb-doping for the ZnO shell. However, in both SCM and SSRM, the ZnO core and the ZnO:Sb shell were clearly differentiated due to their disparity in electrical properties. A strong reduction of the net electron concentration was found for the ZnO:Sb shell in comparison to the nid ZnO core. A reasonable explanation of this difference in carrier density is that the shell layer is compensated by the formation of Sb-related acceptor complexes such as Sb occupying Zn site accompanied by two Zn vacancies (Sb_{Zn}–$2V_{Zn}$), as proposed by Limpijumnong *et al.*,[31] and/or Sb on the O site (Sb_O).[30] So, although the shell was not converted into the p-type layer by Sb doping, a compensation effect of residual donors after Sb introduction has been revealed by SCM/SSRM. From a more quantitative point of view, using the results obtained in SCM measurements, we have determined that the Sb doping compensated more than $10^{18}\,cm^{-3}$ residual donors in the shell part of the ZnO NW. This is an evident proof of the existence of acceptor centers induced by the Sb incorporation. For SSRM results, as we do not know the exact influence of Sb incorporation on the electron mobility properties,

Reuse of AIP Publishing content is subject to the terms at: https://publishing.aip.org/authors/rights-and-permissions. Download to IP: 193.51.38.25 On: Tue, 30 Aug 2016 08:43:15

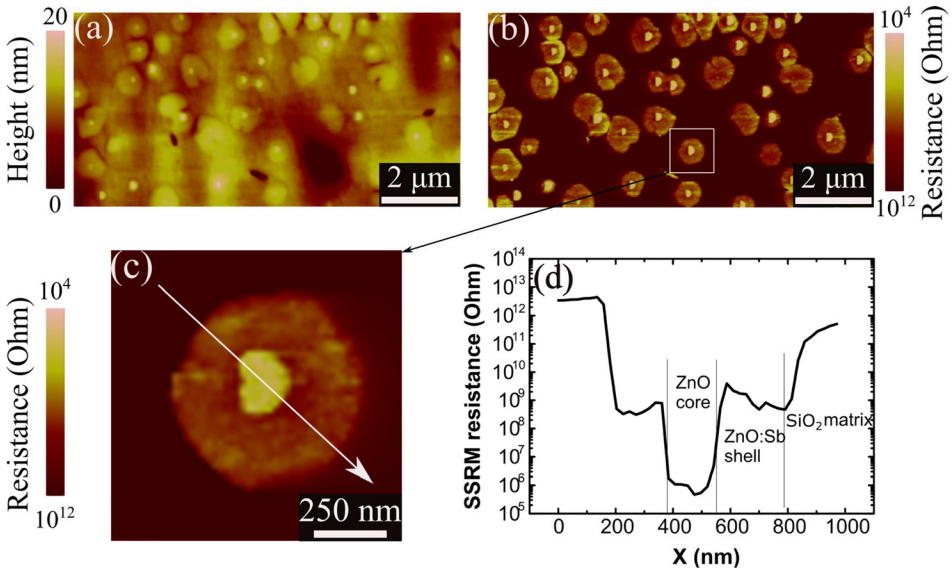

FIG. 3. SSRM result of an area of $10\,\mu m \times 5\,\mu m$ on the ZnO/ZnO:Sb core-shell NW sample. (a) Topography AFM image. (b) SSRM resistance image showing a contrast between the ZnO core and the ZnO:Sb shell. (c) Zoomed-in of the indicated rectangle area in (b). (d) SSRM resistance profile of the arrowed line indicated in (c). Apparently, the shell displays a larger resistance than the core of the NW. A tip force of $\sim 1.5\,\mu N$ and a bias voltage of -3 V on the sample were used.

we did not determine such quantitative results on the compensation degree. However, by taking the compensation degree given by the SCM results, we can estimate that the great amount of Sb (estimated by SIMS) promoted enough defects or contamination to decrease the carrier mobility by more than one order of magnitude.

These results demonstrate the ability of both techniques to accurately characterize the local electrical properties of radial 1D ZnO-based heterostructure properties. Furthermore, considering that p-type doping in ZnO is still under intense study,[5] it is reasonable to imagine that such a structure, which stacks epitaxially grown layers on perfect faceted NWs (i.e., avoiding extended defects and substrate contamination and allowing scanning different growth and doping conditions in the same run), will allow obtaining more useful results on this issue.

In summary, we have utilized SCM and SSRM to characterize ZnO/ZnO:Sb core-shell NWs structures as well as to investigate the Sb doping effect in ZnO. The Sb concentration inside the shell layer was estimated by SIMS on a reference 2D film to be $\sim 6 \times 10^{19}\,cm^{-3}$. As important results, the core-shell difference in terms of electrical properties is well distinguished by both the two techniques. While both parts of the NWs are detected being of n-type conductivity, the ZnO:Sb shell, in consequence of Sb incorporation, shows a relatively low net carrier concentration with respect to the nid ZnO core, which can be ascribed to the formation of Sb-related acceptors compensating the residual donors in the ZnO NW. This work demonstrates that SCM/SSRM can be a direct and effective approach for the characterization of radial semiconductor 1D structures and, in the particular case of this work, for the doping study on the ZnO nanomaterial towards its p-type implementation.

This work was supported by the French program ANR under the Madfiz Project No. ANR-11-NANO-013. Lin Wang would like to acknowledge the financial support from China Scholarship Council. The authors thank Roger Brenier from IML–Université Claude Bernard Lyon 1, for the preparation of SiO_2 solution, David Albertini (INL) for his technical help with the AFM system and Brice Gautier (INL) for helpful discussions on SCM.

[1]U. Özgür, Y. I. Alivov, C. Liu, A. Teke, M. A. Reshchikov, S. Doğan, V. Avrutin, S.-J. Cho, and H. Morkoç, "A comprehensive review of ZnO materials and devices," J. Appl. Phys. **98**, 041301 (2005).
[2]Z. P. Wei, Y. M. Lu, D. Z. Shen, Z. Z. Zhang, B. Yao, B. H. Li, J. Y. Zhang, D. X. Zhao, X. W. Fan, and Z. K. Tang, "Room temperature p-n ZnO blue-violet light-emitting diodes," Appl. Phys. Lett. **90**, 042113 (2007).
[3]M. H. Huang, S. Mao, H. Feick, H. Yan, Y. Wu, H. Kind, E. Weber, R. Russo, and P. Yang, "Room-temperature ultraviolet nanowire nanolasers," Science **292**, 1897 (2001).
[4]M. Law, L. E. Greene, J. C. Johnson, R. Saykally, and P. Yang, "Nanowire dye-sensitized solar cells," Nat. Mater. **4**, 455 (2005).
[5]J. C. Fan, K. M. Sreekanth, Z. Xie, S. L. Chang, and K. V. Rao, "p-Type ZnO materials: Theory, growth, properties and devices," Prog. Mater. Sci. **58**, 874 (2013).
[6]S. B. Zhang, S.-H. Wei, and A. Zunger, "Intrinsic n-type versus p-type doping asymmetry and the defect physics of ZnO," Phys. Rev. B **63**, 075205 (2001).
[7]D. M. Hofmann, A. Hofstaetter, F. Leiter, H. Zhou, F. Henecker, B. K. Meyer, S. B. Orlinskii, J. Schmidt, and P. G. Baranov, "Hydrogen: A relevant shallow donor in zinc oxide," Phys. Rev. Lett. **88**, 045504 (2002).
[8]C. H. Park, S. B. Zhang, and S.-H. Wei, "Origin of p-type doping difficulty in ZnO: The impurity perspective," Phys. Rev. B **66**, 073202 (2002).
[9]A. Janotti and C. G. Van de Walle, "Native point defects in ZnO," Phys. Rev. B **76**, 165202 (2007).
[10]J. G. Lu, P. Chang, and Z. Fan, "Quasi-one-dimensional metal oxide materials—Synthesis, properties and applications," Mater. Sci. Eng., R **52**, 49–91 (2006).
[11]J. Cui, "Zinc oxide nanowires," Mater. Charact. **64**, 43–52 (2012).
[12]P.-C. Chang, Z. Fan, C.-J. Chien, D. Stichtenoth, C. Ronning, and J. G. Lu, "High-performance ZnO nanowire field effect transistors," Appl. Phys. Lett. **89**, 133113 (2006).
[13]G. D. Yuan, W. J. Zhang, J. S. Jie, X. Fan, J. A. Zapien, Y. H. Leung, L. B. Luo, P. F. Wang, C. S. Lee, and S. T. Lee, "p-Type ZnO nanowire arrays," Nano Lett. **8**, 2591 (2008).
[14]G. Wang, S. Chu, N. Zhan, Y. Lin, L. Chernyak, and J. Liu, "ZnO homojunction photodiodes based on Sb-doped p-type nanowire array and n-type film for ultraviolet detection," Appl. Phys. Lett. **98**, 041107 (2011).
[15]O. Hultin, G. Otnes, M. T. Borgström, M. Björk, L. Samuelson, and K. Storm, "Comparing Hall effect and field effect measurements on the same single nanowire," Nano Lett. **16**, 205 (2016).
[16]K. Storm, F. Halvardsson, M. Heurlin, D. Lindgren, A. Gustafsson, P. M. Wu, B. Monemar, and L. Samuelson, "Spatially resolved Hall effect measurement in a single semiconductor nanowire," Nat. Nanotechnol. **7**, 718 (2012).
[17]C. C. Williams, "Two-dimensional dopant profiling by scanning capacitance microscopy," Annu. Rev. Mater. Sci. **29**, 471 (1999).
[18]P. Eyben, M. Xu, N. Duhayon, T. Clarysse, S. Callewaert, and W. Vandervorst, "Scanning spreading resistance microscopy and spectroscopy for routine and quantitative two-dimensional carrier profiling," J. Vac. Sci. Technol., B **20**, 471 (2002).

Reuse of AIP Publishing content is subject to the terms at: https://publishing.aip.org/authors/rights-and-permissions. Download to IP: 193.51.38.25 On: Tue, 30 Aug 2016 08:43:15

[19]E. Latu-Romain, P. Gilet, N. Chevalier, D. Mariolle, F. Bertin, G. Feuillet, and A. Chelnokov, "Surface-induced p-type conductivity in ZnO nanopillars investigated by scanning probe microscopy," J. Appl. Phys. **107**, 124307 (2010).
[20]L. Wang, J. Laurent, J. M. Chauveau, V. Sallet, F. Jomard, and G. Brémond, "Nanoscale calibration of n-type ZnO staircase structures by scanning capacitance microscopy," Appl. Phys. Lett. **107**, 192101 (2015).
[21]L. Wang, J. M. Chauveau, R. Brenier, V. Sallet, F. Jomard, C. Sartel, and G. Brémond, "Access to residual carrier concentration in ZnO nanowires by calibrated scanning spreading resistance microscopy," Appl. Phys. Lett. **108**, 132103 (2016).
[22]N. Hanèche, A. Lusson, C. Sartel, A. Marzouki, V. Sallet, M. Oueslati, F. Jomard, and P. Galtier, "Optical characterization of nitrogen- and antimony-doped ZnO thin layers grown by MOVPE," Phys. Status Solidi B **247**, 1671 (2010).
[23]J. K. Liang, H. L. Su, P. Y. Chuang, C. L. Kuo, S. Y. Huang, T. S. Chan, Y. C. Wu, and J. C. A. Huang, "Origin of p-type conductivity of Sb-doped ZnO nanorods and the local structure around Sb ions," Appl. Phys. Lett. **106**, 212101 (2015).
[24]H. Liang, Y. Chen, X. Xia, Q. Feng, Y. Liu, R. Shen, Y. Luo, and G. Du, "Influence of Sb valency on the conductivity type of Sb-doped ZnO," Thin Solid Films **589**, 199 (2015).
[25]Z. L. Wang and J. Song, Science **312**, 242 (2006).
[26]J. Smoliner, B. Basnar, S. Golka, E. Gornik, B. Löffler, M. Schatzmayr, and H. Enichlmair, "Mechanism of bias-dependent contrast in scanning-capacitance-microscopy images," Appl. Phys. Lett. **79**, 3182 (2001).
[27]R. A. Oliver, "Advances in AFM for the electrical characterization of semiconductors," Rep. Prog. Phys. **71**, 076501 (2008).
[28]H. E. Ruda and A. Shik, "Theoretical analysis of scanning capacitance microscopy," Phys. Rev. B **67**, 235309 (2003).
[29]A. D. L. Bugallo, F. Donatini, C. Sartel, V. Sallet, and J. Pernot, "Metallic core conduction in unintentionally doped ZnO nanowire," Appl. Phys. Express **8**, 025001 (2015).
[30]H. Y. Liu, N. Izyumskaya, V. Avrutin, U. Özgür, A. B. Yankovich, A. V. Kvit, P. M. Voyles, and H. Morkoç, "Donor behavior of Sb in ZnO," J. Appl. Phys. **112**, 033706 (2012).
[31]S. Limpijumnong, S. B. Zhang, S.-H. Wei, and C. H. Park, "Doping by large-size-mismatched impurities: The microscopic origin of arsenic- or antimony-doped p-type zinc oxide," Phys. Rev. Lett. **92**, 155504 (2004).

Reuse of AIP Publishing content is subject to the terms at: https://publishing.aip.org/authors/rights-and-permissions. Download to IP: 193.51.38.25 On: Tue, 30 Aug 2016 08:43:15